Spectrochimica Acta Part A: Molecular and Biomolecular Spectroscopy 115 (2013) 12–21

Contents lists available at SciVerse ScienceDirect

Spectrochimica Acta Part A: Molecular and Biomolecular Spectroscopy

journal homepage: www.elsevier.com/locate/saa

Metal based photosensitizers of tetradentate Schiff base: Promising role in anti-tumor activity through singlet oxygen generation mechanism

S.M. Pradeepa [a], H.S. Bhojya Naik [a,*], B. Vinay Kumar [a], K. Indira Priyadarsini [b], Atanu Barik [b], T.R. Ravikumar Naik [c], M.C. Prabhakara [d]

[a] Department of Studies and Research in Industrial Chemistry, Kuvempu University, Shankaraghatta 577 451, Shimoga, India
[b] Radiation Chemistry Section, Radiation and Photochemistry Division, Bhabha Atomic Research Centre, Mumbai 400 085, India
[c] Department of Organic Chemistry, Indian Institute of Science, Bangalore 560 012, India
[d] Department of Studies and Research in Industrial Chemistry, Sir. M.V. Govt. Science College, Bommanakatte, Bhadravathi 577 302, India

HIGHLIGHTS

- We have synthesized biologically active bivalent (where M = Co, Ni, Cu) complexes.
- The DNA-binding modes of bivalent complexes were studied by different techniques.
- The DNA-photocleavage abilities of bivalent complexes were studied on pUC19 DNA.
- The Quantum yields of $^1O_2$ generation of bivalent complexes were determined.
- The Cytotoxicity of bivalent complexes was performed on A549 lung cancer cell lines.

GRAPHICAL ABSTRACT

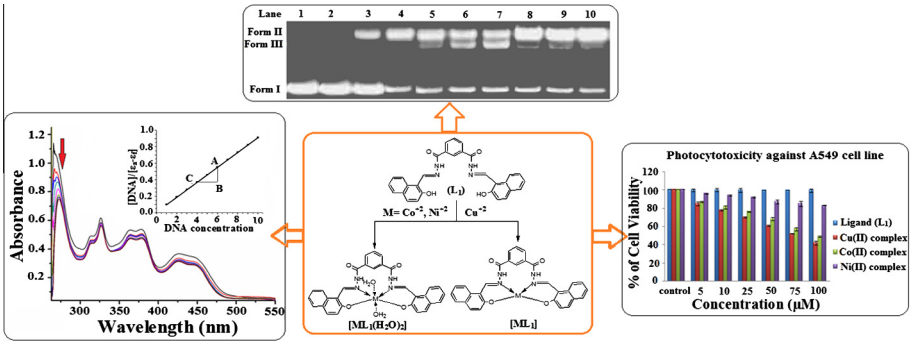

ARTICLE INFO

Article history:
Received 16 December 2012
Received in revised form 27 May 2013
Accepted 4 June 2013
Available online 17 June 2013

Keywords:
Schiff base
Photosensitizer
DNA photocleavage
Singlet oxygen
Cytotoxicity

ABSTRACT

In the present investigation, a Schiff base N^1,N^3-bis[(*Z*)-(2-hydroxynapthyl)methylidene]benzene-1,3-dicarbodihydrazide (L_1) and its Co(II), Ni(II) and Cu(II) complexes have been synthesized and characterized as novel photosensitizing agents for photodynamic therapy (PDT). The interaction of these complexes with calf thymus DNA (CT DNA) has been explored using absorption, thermal denaturation and viscometric studies. The experimental results revealed that Co(II) and Ni(II) complexes on binding to CT DNA imply a covalent mode, most possibly involving guanine N7 nitrogen of DNA, with an intrinsic binding constant K_b of $4.5 \times 10^4\ M^{-1}$ and $4.2 \times 10^4\ M^{-1}$, respectively. However, interestingly, the Cu(II) complex is involved in the surface binding to minor groove via phosphate backbone of DNA double helix with an intrinsic binding constant K_b of $5.7 \times 10^4\ M^{-1}$. The Co(II), Ni(II) and Cu(II) complexes are active in cleaving supercoiled (SC) pUC19 DNA on photoexposure to UV–visible light of 365 nm, through $^1O_2$ generation with quantum yields of 0.28, 0.25 and 0.30, respectively. Further, these complexes are cytotoxic in A549 lung cancer cells, showing an enhancement of cytotoxicity upon light irradiation.

Introduction

Photodynamic therapy (PDT) is an emerging field of medicine as a treatment modality for variety of cancers, utilizes photosensitizers (PSs) and light. During PDT, a photosensitizing agent is activated by light of specific wavelength and produces reactive oxygen species (ROS) which oxidize cell components leading to cell death [1–3]. A large number of PSs reported are the organic molecules, such as dyes, porphyrins, phthalocyanines, and their derivatives. However, many of the studied PSs are not much stable against light, which alter their potential to absorb light during

* Corresponding author. Tel./fax: +91 8282 257302.
E-mail address: hsb_naik@rediffmail.com (H.S. Bhojya Naik).

1386-1425/$ - see front matter © 2013 Elsevier B.V. All rights reserved.
http://dx.doi.org/10.1016/j.saa.2013.06.009

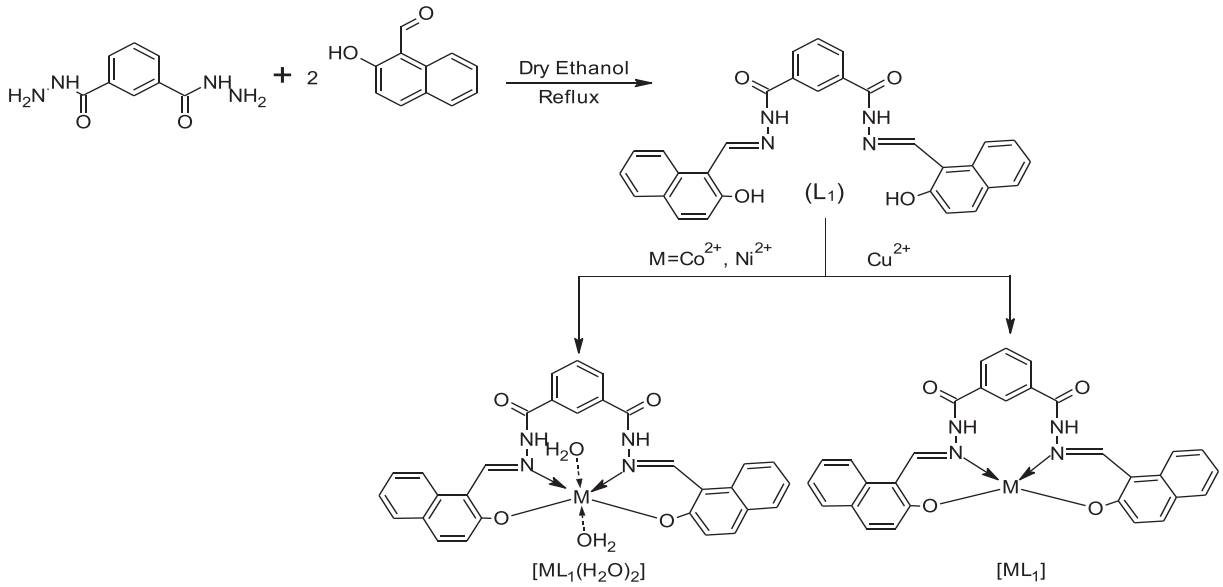

Scheme 1. Synthesis of N'^1,N'^3-bis[(*Z*)-(2-hydroxynapthyl)methylidene] benzene-1,3-dicarbodihydrazide (L_1) and its metal complexes.

illumination, resulting in a decreased efficiency of production of excited molecules [4–7]. The coordination compounds have become an integral part of many aspects of medicine today. Success of cisplatin as a well-organized photosensitizer agent has drawn the attention of many active bioinorganic chemists towards developing transition metal complexes with superior efficiency [8–12]. For example, the complexes of ruthenium(II) and platinum(II) can be the proficient photosensitizers to induce singlet oxygen [13,14]. So, design, synthesis of metal complexes and study of their DNA photocleavage activity is of great scope in PDT [15–17].

In this direction, Schiff base complexes have played a major role in the development of PSs [18–22]. Due to synthetic flexibility, selectivity and sensitivity towards a variety of metal atoms, the Schiff bases formed a number of metal complexes and they have been extensively studied as PSs. It has been reported that the transition metal complexes of different-donor Schiff base ligands are efficient photo-cleavers of DNA on UV–visible light irradiation [23–25]. Furthermore, numerous metal complexes of Schiff bases derived from salicylaldehyde and amino acid [26–32] and reduced salicylidene amino acid [33–35] were already reported and some of them have been confirmed to be efficient DNA cleavers [36–38] and as novel tumor chemotherapeutic and tumor radio imaging agents [39].

The present work stems from our interest in developing the chemistry of transition metal complexes of various organic heterocyclic ligands as binders and efficient photocleavers of DNA, considering the biocompatibility of both the metal and the ligands [40–42]. Recent report from our laboratory have shown that, Co(II), Ni(II) and Cu(II) complexes derived from a Schiff base N'^1,N'^3-bis[(*E*)-(5-bromo-2-hydroxyphenyl)methylidene]benzene-1,3-dicarbohydrazide are efficient photocleavers of DNA via formation of $^1O_2$ and exhibiting significantly high photocytotoxicity upon irradiation with visible light in A549 cells [43].

Herein, we present the synthesis and characterization of a Schiff base ligand (L_1) and its Co(II), Ni(II) and Cu(II) complexes (Scheme 1). A series of physical methods like absorption spectral, thermal denaturation studies, and viscosity measurements have been used to probe the interactions of the bivalent metal complexes with CT DNA. Furthermore, the photoinduced DNA cleavage activity, quantum yield of singlet oxygen generation and the related photocytotoxicity against A549 cancer cell lines was experimentally explored. The remarkable DNA binding affinity, efficient photocleavage and significant photocytotoxicity were resulted that the complexes would have potential application as new class of PSs for PDT of cancer.

Experimental

Materials

All chemicals required for the synthesis were of analytical grade, and procured from HiMedia Laboratories Pvt. Ltd. Metal salts ($CoCl_2{\cdot}6H_2O$, $NiCl_2{\cdot}6H_2O$ and $CuCl_2{\cdot}2H_2O$), 2-hydroxynaphthalene-1-carbaldehyde, sodium azide (NaN_3), 3-(4,5-Dimethylthiazol-2-yl)-2,5-diphenyltetrazoliumbromide (MTT) were purchased from Sigma Chemical Co., U.S.A., E. Merck, Germany, Sarabhai Merck Company, India and used without further purification. Tris–HCl was purchased from Merck (India). Calf thymus (ds)DNA and supercoiled (SC) pUC19 DNA were purchased from Bangalore Genie (India), Agarose (molecular biology grade) and ethidium bromide were purchased from Himedia. Tris–HCl buffer solution used for binding and cleavage studies was prepared using deionised double distilled water.

Physical measurements

The melting points were determined by open capillary methods and are uncorrected. The UV–visible spectra were recorded on a Shimadzu model impact 1650 UV–visible double beam spectrometer and the FT-IR spectra on a Shimadzu model impact 8400S FT-IR spectrometer (KBr pellets, 3 cm^{-1} resolution), ^{1}HNMR spectra on a Bruker 400 MHz. The EPR spectra was measured on a VARIAN, USA E-112 ESR X-band Spectrometer and Mass spectra were recorded on LCMS Shimadzu, Japan 800 MHz spectrometer. Magnetic measurements were carried out by the Gouy method at room temperature (28 ± 2 °C) using $Hg[Co(SCN)_4]$ as calibrant. Elemental analyses were done on Vario EL.CHNOS elemental analyser. Viscometric measurements were studied by semi micro dilution capillary viscometer (Viscomatic Fica MgW) with a thermostated bath D40S.

Synthesis of Schiff base ligand (L_1)

A solution of benzene-1,3-dicarbohydrazide (0.01 mol) in anhydrous ethanol (50 mL) was added drop wise to the ethanolic

solution (50 mL) of 2-hydroxynaphthalene-1-carbaldehyde (0.02 mol) in presence of acetic acid catalyst and the mixture was heated under reflux for 5–6 h (Scheme 1). The resulting solution was concentrated to half of its initial volume and then cooled to room temperature. The obtained yellow precipitate was separated by filtration, washed with ethanol and dried in a vacuum desiccator. Yield: 89%. Color: yellow. m.p: 306–308 °C. Anal. (%) Calc. for [$C_{30}H_{22}N_4O_4$]: C, 71.70; H, 4.41; N, 11.15. Found: C, 71.72; H, 4.40; N, 11.17. LC–MS (*m*/*z*) 503 $[M+H]^+$. IR (KBr, cm^{-1}): 3483 (—OH), 1738 (C=O), 1650 (C=N), 3058 (N—H), 1270 (N—N); ^1H NMR (DMSO-d_6, 400 MHz, δ ppm): 12.72 (s, O—H, 2H), 12.41 (s, N—H, 2H), 9.53 (s, —CH=N, 2H), 7.24–8.62 (m, Ar—16H). UV–vis in DMF [λ_{max}/nm (ε/M^{-1} cm^{-1})]: 378 (8630), 326 (9780), 312 (7140), 268 (8850).

Synthesis of Co(II), Ni(II) and Cu(II) complexes

An ethanolic solution of ligand (L_1) (0.01 mol) and respective metal chloride salt (0.01 mol) was refluxed for 2–3 h under nitrogen (Scheme 1). The complex was precipitated by adding distilled water. The separated complex was filtered, washed with water, then with hot alcohol and finally dried in vacuum desiccator over P_2O_5.

Co(II) complex

Yield: 75%; Color: brown; m.p.:>360 °C; Anal. (%) Calc. for [$C_{30}H_{24}CoN_4O_6$]: C, 60.51; H, 4.06; N, 9.41. Found: C, 60.52; H, 4.05; N, 9.39; LC–MS (*m*/*z*) 596 $[M+H]^+$. IR (KBr, cm^{-1}): 3410 (OH coordinated H_2O), 1738 (C=O), 1638 (C=N), 545 (M—O), 435 (M—N); UV–vis in DMF [λ_{max}/nm (ε/M^{-1} cm^{-1})]: 470 (7850), 436 (8260), 380 (5740), 342 (8633), 326 (8600), 278 (20140).

Ni(II) complex

Yield: 70%; Color: greenish; m.p.:>360 °C; Anal. (%) Calc. for [$C_{30}H_{24}NiN_4O_6$]: C, 60.53; H, 4.06; N, 9.41. Found: C, 60.51; H, 4.07; N, 9.39; LC–MS (*m*/*z*) 597 $[M+H]^+$. IR (KBr, cm^{-1}): 3425 (OH coordinated H_2O), 1737 (C=O), 1612 (C=N), 548 (M—O), 442 (M—N); UV–vis in DMF [λ_{max}/nm (ε/M^{-1} cm^{-1})]: 458 (5620), 424 (5965), 377 (8660), 362 (8630), 325 (9780), 270 (14740).

Cu(II) complex

Yield: 73%; Color: greenish; m.p.:>360 °C; Anal. (%) Calc. for [$C_{30}H_{20}CuN_4O_4$]: C, 63.88; H, 3.57; N, 9.93. Found: C, 63.87; H, 3.55; N, 9.95; LC–MS (*m*/*z*) 565 $[M+H]^+$. IR (KBr, cm^{-1}): 1738 (C=O), 1600 (C=N), 550 (M—O), 448 (M—N); UV–vis in DMF [λ_{max}/nm (ε/M^{-1} cm^{-1})]: 440 (7700), 419 (8690), 339 (7290), 325 (7140), 279 (11580).

DNA-binding experiments

The DNA-binding propensity and photoinduced cleavage experiments of the complexes were performed at an ambient temperature. Calf thymus DNA binding experiments were performed using Tris–HCl and phosphate buffers. The absorption spectral and viscosity experiments were carried out in 5 mM Tris–HCl buffer (5 mM Tris (hydroxymethyl)aminopropane, pH 7.2, 50 mM NaCl). The DNA melting experiments were performed using phosphate buffer (1 mM phosphate, 2 mM NaCl, pH 7.0). The DNA was found to be free of protein impurity, as evidenced from the ratio of the absorbance values of the DNA at 260 and 280 nm in Tris–HCl buffer as 1.9:1.8. The DNA concentration (in the base pairs) was determined by electronic absorption spectroscopy using a molar absorption coefficient value of 6600 M^{-1} cm^{-1} at 260 nm for CT DNA [44]. UV–visible absorption titration experiments were performed by varying the CT DNA concentration (0–50 μM) and maintaining the complex concentration constant. Correction was made for the absorbance of DNA itself. The spectra were recorded after equilibration for 5 min, allowing the complexes to bind to the CT DNA. The intrinsic binding constant (K_b) for interaction of the complexes with CT DNA was determined from a plot of [DNA]/(ε_a–ε_f) versus [DNA] using absorption spectral titration data and the following equation (1).

$$[DNA]/(\varepsilon_a - \varepsilon_f) = [DNA]/(\varepsilon_b - \varepsilon_f) + 1/K_b(\varepsilon_a - \varepsilon_f) \quad (1)$$

where [DNA] is the concentration of DNA, the apparent absorption coefficients ε_a, ε_f and ε_b correspond to A_{obsd}/[complex], the extinction coefficients for the free metal complex and the extinction coefficient for the metal complex in the fully bound form, respectively. The K_b value is given by the ratio of the slope to the intercept.

Viscometric titration experiments were performed using a semi micro dilution capillary viscometer at room temperature. The flow time was measured with an automated timer, and each sample was measured three times, and an average flow time was calculated. The resulting data are presented by plotting (η/η_0) vs. [complex]/[DNA], where η is the viscosity of DNA in the presence of complex and η_o is the viscosity of DNA alone [41,45].

DNA thermal denaturation studies were carried out by monitoring the absorption intensity of the CT DNA at 260 nm varying the temperature from 40–80 °C, both in the absence and presence of the complexes in 1 mM phosphate buffer (pH 7.0) [46,47].

DNA cleavage experiments

The cleavage of supercoiled pUC19 DNA (0.5 μL, 0.5 μg) to other forms such as nicked circular and linear conformations was studied by agarose gel electrophoresis using Co(II), Ni(II) and Cu(II) complexes in a 50 mM Tris-(hydroxymethyl)methane–HCl (Tris–HCl) buffer (pH 7.2) containing 50 mM NaCl. The DNA photocleavage reactions were carried out by irradiating the complexes in micro centrifuge tubes at 365 nm for 30 min. at room temperature. After light exposure, each sample was incubated for 1.0 h at 37 °C and analyzed for the photocleaved products using agarose gel electrophoresis. The samples after incubating in a dark chamber were immediately added to the loading buffer containing 20% bromophenol blue, 0.20% xylene cyanol, and 25% glycerol (2.5 μL), and the solution was finally loaded on 0.7% agarose gel containing 1.0 μg/mL ethidium bromide. For quenching singlet oxygen the mechanistic studies were carried out using different additives (NaN_3, 38 μM) and scavenging hydroxyl radicals (DMSO, 4 μL) prior to the addition of the complexes. Using TBE (Tris–borate EDTA) buffer electrophoresis was carried out for 2.5 h at 50 V. After completion of the electrophoresis the separated bands were visualized by UV light and then photographed. The amount of DNA cleavage exhibited by the complexes was calculated from the intensities of the bands using a UVITEC Gel Documentation System [42,48].

Quantum yield of $^1O_2$ generation

The reaction of $^1O_2$ with 1,3-diphenylisobenzofuran (DPBF, Scheme 2) was adopted to evaluate the quantum yield of $^1O_2$ generation by Co(II), Ni(II) and Cu(II) complexes. A sequence of 2 mL of air-saturated DMSO solutions containing DPBF (20 μM) and complexes, of which the absorbance at 470, 458 and 440 nm originating from the absorption of Co(II), Ni(II) and Cu(II) complexes was adjusted to the same (OD_{470} nm, OD_{458} nm and OD_{440} nm = 0.22), were separately charged into an opened 1 cm path quartz cuvette and illuminated with light of 470 nm, 458 nm and 440 nm (obtained from a Shimadzu model impact 1650 UV–visible double beam spectrophotometer, 2.0 nm of slit width). The consumptions of DPBF were followed by monitoring its loss of absorbance at 417 nm (λ of irradiation = 470, 458 and 440 nm) at different irradiation time. $[Ru(bpy)_3]^{2+}$ (bpy = 2,2′-bipyridine) was used as

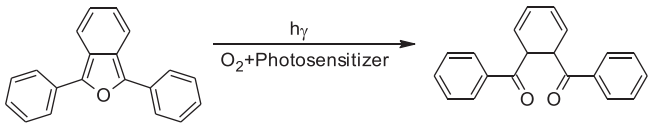

Scheme 2. The reaction of DPBF with singlet oxygen.

standard, whose $^1O_2$ generation quantum yield was determined to be 0.81 in air saturated methanol [49].

Antitumor activity

Antitumor activity *in vitro* was evaluated using a system based on the tetrazolium salt 3-(4,5-dimethyl-2-thiazoyl)-2,5-diphenyl-tetrazolium bromide (MTT). Lung cancer A549 cell line was cultured in Dulbecco's modified Eagle's medium (Thermo Scientific HyClone, Logan, USA) supplemented with 10% (v/v) fetal bovine serum (FBS) in 5% CO_2 atmosphere at 37 °C, respectively. For cell viability assay, the cancer cells were plated at a density of 104 cells/well in 96-well plates and incubated for 24 h. The medium was removed, and complex solutions were added into a new medium without FBS to the required final concentrations between 5 μM and 200 μM. The untreated A549 cells were used as a control.

After 72 h of incubation, 10 μL of a stock MTT solution was added to give a final concentration of 0.5 mg/mL and incubated for a further 4 h. Then, the medium was replaced with 100 μL of pure dimethyl sulfoxide and the absorbance of the dark blue formazan was measured with an ELISA plate reader at 550 nm. Cell viability = $(A_{sample}/A_{control}) \times 100\%$. After 72 h of incubation with complexes, 30 μL of washed cell suspension was mixed thoroughly with 30 μL of trypan blue solution (0.4%) and allowed to stand for 3 min. at room temperature. The total number of cells and the number of blue-stained cells (dead cells) were counted using a microscope [50].

Results and discussion

A Schiff base ligand (L_1) was obtained by the reaction of 2-hydroxynaphthalene-1-carbaldehyde (0.02 mol) and benzene-1,3-dicarbohydrazide (0.01 mol) in ethanol in presence of acetic acid as catalyst. The metal complexes were prepared by a direct reaction of respective metal salts and the ligand in 1:1 M ratio, using methanol as the reaction medium (Scheme 1). The Schiff base ligand (L_1) and its complexes were characterized using IR, UV–visible, ^{1}HNMR, EPR and mass spectral studies. The compositions of the complexes were confirmed by elemental analysis, conductivity measurements and mass spectral studies. The experimentally calculated analytical data of compounds are consistent with their proposed molecular formulae. The molar conductivity measurement in DMF at 10^{-3} M concentration gave a Λ_o value in the range of 67–73 $ohm^{-1}\,mol^{-1}\,cm^{-1}$ at 300 k, suggesting that the complexes are non-electrolytic in nature. The complexes are stable towards air, light and moisture and soluble in DMSO, DMF and in buffer solution.

Spectroscopic studies

In the IR spectra of complexes, the observed band at 3483 cm^{-1}, is due to phenolic —OH and the band at 1650 cm^{-1}, is due to C=N group of the free Schiff base ligand (L_1), disappeared upon complexation, indicates that phenolic —OH and C=N of the ligand coordinate to the metal through oxygen via deprotonation and through azomethine nitrogen. The presence of broad stretching vibrations in the range of 3402–3452 cm^{-1} can be attributed to coordinated water molecules [51–55], in Co(II) and Ni(II) complexes, respectively. The unaltered position of the υ(C=O) (carbonyl) and υ(N—H) confirms non-involvement of these groups in coordination. The new bands observed in the region 545–550 cm^{-1} and 435–450 cm^{-1}, have been assigned for υ(M—O) and υ(M—N) bonds, respectively.

The electronic spectra of the free dihydrazone ligand (L_1) in DMF solution exhibit characteristic bands at 268 nm (ε_{max}, 8850 $M^{-1}\,cm^{-1}$), 312 nm (ε_{max}, 7140 $M^{-1}\,cm^{-1}$), 326 nm (ε_{max}, 9780 $M^{-1}\,cm^{-1}$) and 378 nm (ε_{max}, 8630 $M^{-1}\,cm^{-1}$). The bands present at 268–326 nm is assigned to intraligand π–π^* transition while the band at 378 nm is assigned to the n–π^* transition which is characteristic of azomethine (C=N) function of the Schiff base [56]. The electronic spectra of the complexes show two to four bands in the region 270–470 nm. While the band in the region 420–440 nm is assigned to ligand band at 378 nm, the additional bands in the region 270–380 nm are assigned to another ligand bands appearing in the region 268–326 nm. On the other hand, the appearance of a new bands with high molar extinction coefficient in the region 470–440 nm for Co(II), Ni(II) and Cu(II) complexes, may be assigned to ligand to metal charge transfer (LMCT) transitions [57].

The magnetic moments of the complexes were recorded at room temperature. The magnetic measurement for Co(II) complex showed magnetic moment value of 5.12 BM which is well within the range of 4.3–5.2 BM and Ni(II) complex showed the magnetic moment value of 3.17 BM within the range of 2.8–3.5 BM suggesting [58,59] consistency with their octahedral environment. The magnetic moment value of 1.87 BM for Cu(II) complex suggests the four coordinated square planar geometry [60–63], which further supported by their electronic spectral data.

The mass spectrum of L_1 supported the suggested structure of the ligand, revealing a molecular ion $[M+H]^+$ peak at m/z at 503, consistent with the molecular weight of the ligand (Supplementary file, Fig. S1). Further, the mass spectral result of the complexes provide good evidence for their proposed molecular formulae, by observing the $[M+H]^+$ peaks at m/z 596, 597 and 565 equivalent to its molecular weight of 595, 596 and 564 for Co(II), Ni(II) and Cu(II) complexes respectively, confirms the stoichiometric composition of $[M(L_1)(H_2O)_2]$ type for Co(II) and Ni(II) complexes and $[M(L_1)]$ type for Cu(II) complex respectively (Supplementary file, Figs. S2–S4).

^{1}H NMR spectra

The ^{1}H NMR spectra of Schiff base ligand (L_1) was recorded in dimethylsulfoxide ($DMSOd_6$) solution using Me_4Si (TMS) as internal standard. The down field shift of the —OH proton in the Schiff base ligand (L_1) resonates at 12.72 ppm in its ^{1}H NMR spectrum indicates that the —OH proton of the ligand are probably involved in the formation of strong intramolecular hydrogen bonding. The ^{1}H NMR spectrum of the ligand exhibits characteristic azomethine proton signal at 9.53 ppm. The ligand [L_1] showed —NH proton at 12.41 ppm, aromatic ring protons at 7.24–8.62 ppm. The ^{1}H NMR spectra of the complexes cannot be obtained due to interference in their paramagnetic properties.

EPR studies

The solid state EPR spectra of the Cu(II) complex was recorded in X-band frequencies as shown in Fig. 1. At liquid nitrogen temperature the complex exhibits well defined single isotropic feature near $g = 2.08$. Such isotropic lines are usually the results of intermolecular spin exchange, which broaden the lines. This intermolecular type of spin exchange is caused by the strong spin coupling which occurs during a coupling of two paramagnetic species. The anisotropic g-values have been calculated by kneubuhl's method [64–66]. The $G = (g_{\parallel} - 2)/(g_{\perp} - 2)$, which measure the

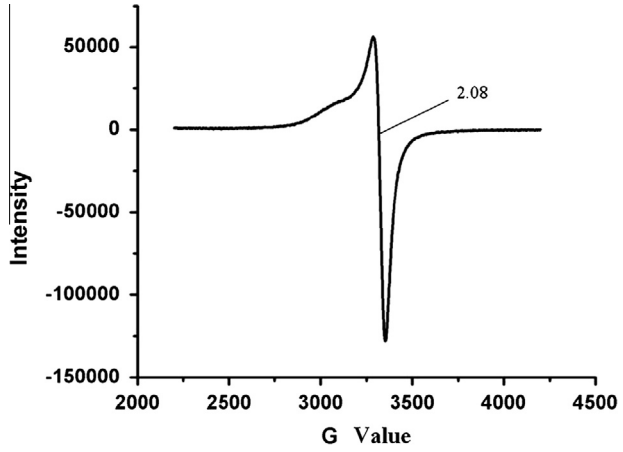

Fig. 1. Solid state X-band EPR spectra of Cu(II) complex at room temperature.

exchange interaction between the copper centers in polycrystalline samples, have been calculated. According to Hathaway [67], if $G > 4$, the exchange interaction is negligible. A value of $G < 4$, indicates considerable exchange interaction in the solid complexes. Therefore, the intermolecular spin exchange has happened by the strong spin coupling of two paramagnetic species of the Cu(II) complex.

DNA binding properties of the complexes

Electronic absorption spectroscopy is widely employed to determine the DNA binding affinity of metal complexes. It is well known that the transition metal based complexes can bind to DNA via covalent and/or non-covalent interactions [68]. Generally, covalent interactions include coordination to the DNA base, sugar, and phosphate moieties [69]. Non-covalent interactions include binding to minor groove, major groove, sugar–phosphate backbone, and intercalation between the bases and three way junction [70]. It has been reported that, the two labile chloride ions (or one or more water molecules) of the transition metal complexes are replaced by a nucleophile on DNA, usually a nitrogenous base such as guanine N7, leading to a strong covalent bonding of the complexes

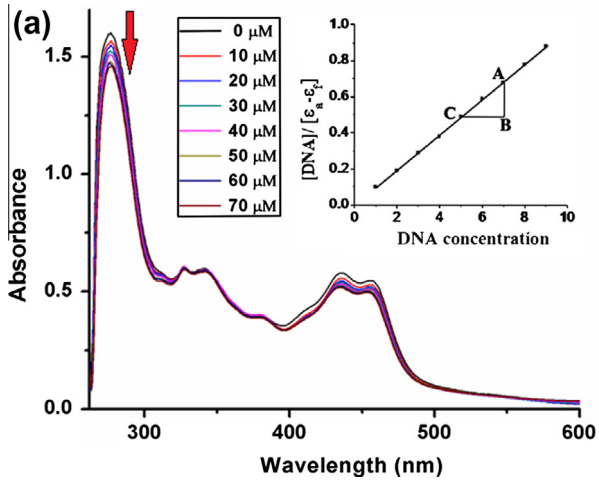

Fig. 2a. Absorption spectral traces of $[Co(L_1)(H_2O)_2]$ complex in *Tris*–HCl buffer upon the addition of CT-DNA. $[Co(L_1)(H_2O)_2] = 0.5$ μM. Arrow shows the absorbance changing upon increase of DNA concentration. The inner box representing the concentration corresponding to each curve. The inner plot of $[DNA]/(\varepsilon_a - \varepsilon_f)$ vs [DNA] for the titration of DNA with Co(II) complex, $K_b = 4.5 \times 10^4\ M^{-1}$.

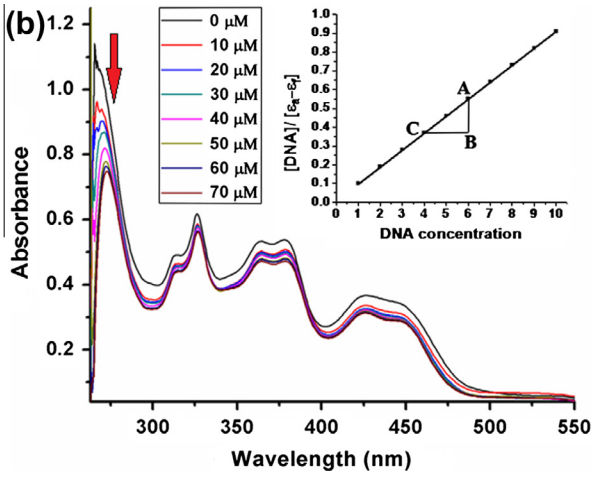

Fig. 2b. Absorption spectral traces of $[Ni(L_1)(H_2O)_2]$ complex in *Tris*–HCl buffer upon the addition of CT-DNA. $[Ni(L_1)(H_2O)_2] = 0.5$ μM. Arrow shows the absorbance changing upon increase of DNA concentration. The inner box representing the concentration corresponding to each curve. The inner plot of $[DNA]/(\varepsilon_a - \varepsilon_f)$ vs [DNA] for the titration of DNA with Ni(II) complex, $K_b = 4.2 \times 10^4\ M^{-1}$.

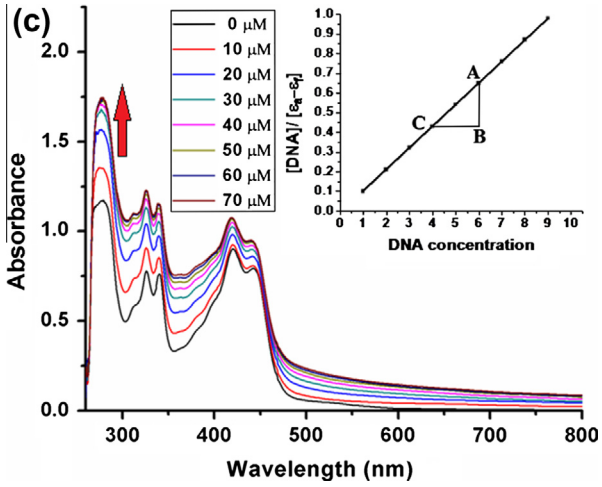

Fig. 2c. Absorption spectral traces of $[Cu(L_1)]$ complex in *Tris*–HCl buffer upon the addition of CT-DNA. $[Cu(L_1)] = 0.5$ μM. Arrow shows the absorbance changing upon increase of DNA concentration. The inner box representing the concentration corresponding to each curve. The inner plot of $[DNA]/(\varepsilon_a - \varepsilon_f)$ vs [DNA] for the titration of DNA with Cu(II) complex, $K_b = 5.7 \times 10^4\ M^{-1}$.

with DNA [69]. On the other hand, structurally complete intercalation of complexes of dihydrazone type ligands between a set of adjacent base pairs is sterically impossible [71], but have the potential to bind to DNA non-covalently, via major/minor groove.

The electronic absorption spectra of Co(II), Ni(II) and Cu(II) complexes in aqueous buffer media both in the absence and the presence of CT-DNA are given in Fig. 2a–c, respectively. The present bivalent complexes do not exhibit any intense d–d transition band to monitor their interaction with DNA. So, the intense ligand based (π–π^*) absorption bands are used to monitor the interaction of the complexes with calf thymus DNA. On the addition of CT DNA, the bivalent complexes show a red and blue shift (3–5 nm) accompanied by a change in intensity of the bands at 270–280 nm. The absorption band of Co(II) complex at 278 nm, exhibited hypochromism of about 18%, with no red/blue shift. Similarly, Ni(II) complex exhibits an evident hypochromism of about 23.6% with significant red shift of 5 nm at 270 nm and Cu(II) complex

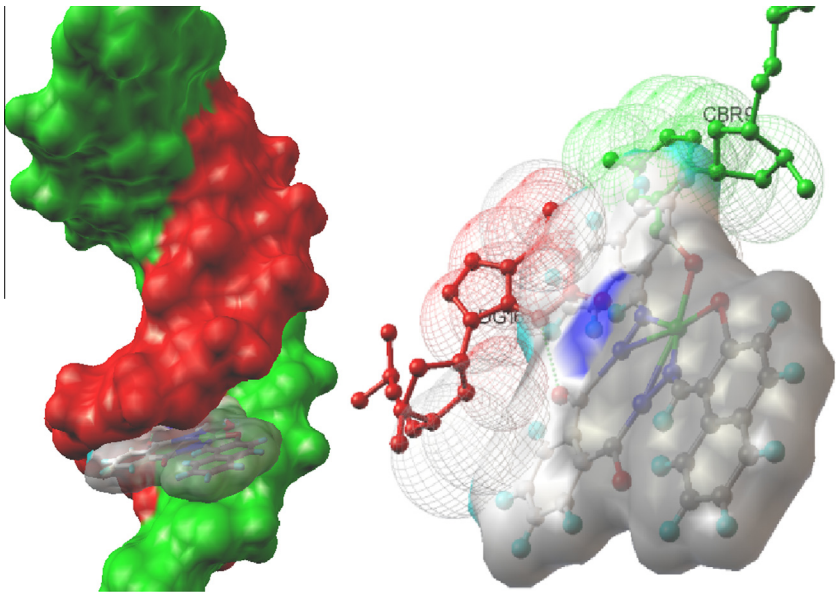

Fig. 3. View of the energy minimized docked structures of Cu(II) complex, with d(CGCGAATTCGCG)$_2$.

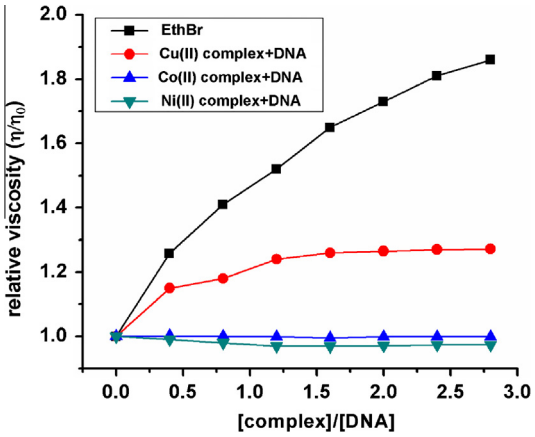

Fig. 4. Effects of increasing amount of Co(II), Ni(II) and Cu(II) complexes on the relative viscosity of CT-DNA at 25 ± 0.1 °C.

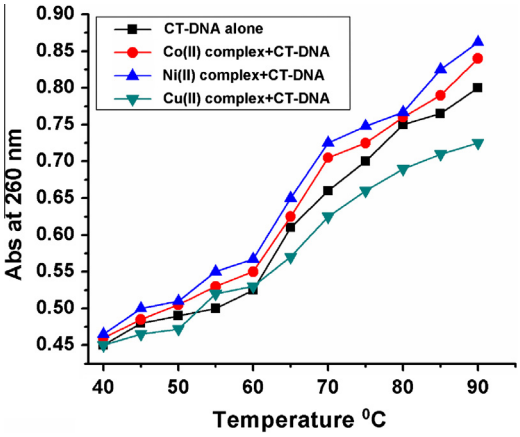

Fig. 5. Melting curves of CT-DNA in the presence and absence of Co(II), Ni(II) and Cu(II) complexes.

exhibits an evident hyperchromism of about 25% with a slight blue shift of 3 nm at 279 nm, respectively. This reveals that the Co(II) and Ni(II) complexes are coordinated presumably to DNA base such as guanine (N7) forming a metal-nitrogen chromophore and are more distorted obviously, due to the presence of octahedral geometry with coordinated water molecules. While the spectral changes exhibited by Cu(II) complex are typical of complexes bound to DNA through non-covalent interaction presumably through groove binding, mainly because of the square planar geometry associated with no coordinated labile groups.

In order to quantify the extent of DNA binding the intrinsic binding constant K_b of the bivalent complexes were determined and it is found to be $4.5 \times 10^4\ M^{-1}$, $4.2 \times 10^4\ M^{-1}$, $5.7 \times 10^4\ M^{-1}$ for Co(II), Ni(II) and Cu(II) complexes, respectively. The observed K_b values are much lower than those observed for typical classical intercalator (EthBr, K_b, $1.4 \times 10^6\ M^{-1}$ in 25 mM Tris–HCl/40 mM NaCl buffer, pH 7.9) and partially intercalating metal complexes ($[Ru(bipy)_2(dppz)]^{2+}$, dppz = dipyrido-[3,2-d: 2′,3′-*f*]-phenazine, $K_b > 10^6\ M^{-1}$) bound to CT DNA suggests that the Co(II) and Ni(II) complexes bound to DNA via covalent whereas Cu(II) through non-covalent interactions.

An explanation for higher K_b value of Cu(II) complex is apparently that copper is 'borderline' metal which show high affinity for both nucleobases and phosphate, but the steric clashes with DNA exterior caused by the ligand bound to Cu(II) dictates its DNA-binding mode to be surface binding to minor groove [72–77].

Due to the variations observed in the absorption spectral study of Cu(II) complex, the molecular docking calculations have been carried out in order to gain further insight into the binding of Cu(II) complex with d(CGCGAATTCGCG)$_2$ [78]. The docking studies showed that, the Cu(II) complex possess interaction with phosphate backbone with additional hydrogen bonding (2.9–2.7 Å) which might play a key role in the enhanced binding constant of Cu(II) complex as compared to other complexes. Furthermore, the Cu(II) complex showed highest affinity −22.10 kcal/mol docking energy, 2.3×10^{-16} estimated inhibition constants with an RMSD of 0.4. As depicted in Fig. 3, the Cu(II) complex is completely enfolded in the entire binding pocket of ds-DNA and interact along the minor groove of DNA. This is possibly due to the absence of any coordinated water molecules. Thus, the results obtained from molecular docking studies were paralleled to the above UV–visible spectroscopic data such as hyperchromism and blue-shift of Cu(II) complex in the presence of DNA.

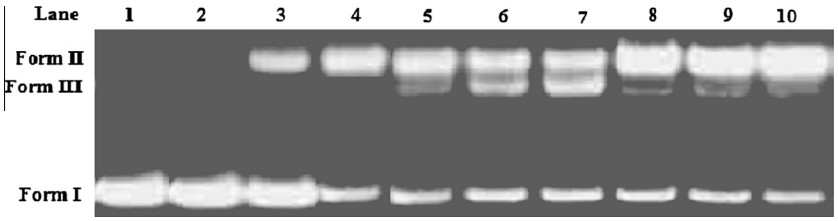

Fig. 6. Gel electrophoresis diagram of the control experiments using SC pUC19 DNA (0.5 μg), metal complexes and other additives at 365 nm for an exposure time of 1 h. Lane 1: DNA control; lane 2: DNA + NaN_3 (38 μM) + Co(II)/Ni(II)/Cu(II) complexes; lane 3: DNA + D_2O (14 μL) + Co(II)/Ni(II)/Cu(II) complexes; lane 4: DNA + DMSO (4 μL) + Co(II)/Ni(II)/Cu(II) complexes; lane 5: DNA + 40 μM Co(II) complex; lane 6: DNA + 60 μM Co(II) complex; lane 7: DNA + 40 μM Ni(II) complex; lane 8: DNA + 60 μM Ni(II) complex; lane 9: DNA + 40 μM Cu(II) complex; lane 10: DNA + 60 μM Cu(II) complex.

Viscosity measurements

Viscometric titration experiments further clarified the binding modes of complexes with CT-DNA. Hydrodynamic measurements that are perceptive to length change (for example, viscosity, sedimentation) are regarded as the most decisive tests of binding in solution in the absence of crystallographic structure data [79]. The viscosity of DNA is enhanced significantly due to complete or partial intercalation of drugs into the DNA base stacking but it is slightly reduced or shows no effect on the relative viscosity by electrostatic/groove or covalent binding of molecules [80–82]. Further, an intercalator like ethidium bromide shows a significant increase in the relative viscosity of the CT DNA solution due to an increase in the overall DNA contour length on binding to DNA [83]. To throw further light on the DNA binding mode, the viscometric titration experiments were carried out on CT DNA by varying the concentration of added complex. The relative viscosity of DNA is decreases strongly and then remains constant with the addition of increasing amounts of Co(II) and Ni(II) complexes, which parallels the highest ΔT_m values observed for them. Thus, the extensive diadduct formation by these complexes, as discussed above, shortens the effective length of DNA by forming bends or kinks on the DNA double helix [84]. However, interestingly, a slight increase in the viscosity of the DNA is observed for Cu(II) complex, which parallels the highest K_b and lowest ΔT_m values observed for it, indicating groove binding nature of the complex to CT DNA (Fig. 4). It appears that the effective lengthening of DNA duplex occurs on groove binding of the Cu(II) complex as illustrated above. A comparison of the viscosity data with intercalator ethidium bromide indicates a covalent binding mode for Co(II) and Ni(II) complexes and a groove binding mode for Cu(II) complex, respectively.

Thermal denaturation studies

The DNA melting experiments were carried out to investigate the effect of DNA duplex stability due to binding of the complexes. Duplex DNA at its melting temperature unwinds to give single-strand DNA, thus increasing its absorbance at 260 nm [85]. Thus, the helix to coil transition temperature can be determined by monitoring the absorbance of DNA at 260 nm as a function of temperature. The thermal denaturation profile of DNA in the absence and presence of Co(II), Ni(II) and Cu(II) complexes is provided in Fig. 5. A change in the DNA melting temperature (ΔT_m) was observed on addition of the complexes to CT DNA and the absorbance of the solutions at 260 nm monitored. The observation of DNA melting curves with high ΔT_m values for Co(II) and Ni(II) complexes [Co(II), 5.5 ± 1 °C; Ni(II), 6.1 ± 1 °C; Fig. 5) reveals that these complexes are involved in strong binding to DNA implying that the complex bound DNA is more difficult to melt than the unlabelled DNA [86]. Certain mononuclear $[Ru(L)(H_2O)_2]$ complexes are known to exhibit positive ΔT_m values, suggesting stronger covalent cross-linking of two DNA strands by the difunctional diaquo complexes. A similar higher positive ΔT_m values observed for Co(II) and Ni(II) complexes, indicating primarily DNA covalent-binding property of the complexes. Further, interestingly, the Cu(II) complex possesses a ΔT_m value (ΔT_m = 2.5 ± 1 °C) lower than the Co(II) and Ni(II) complexes. It is also possible that the large difference in ΔT_m values may be due to a difference in binding geometry of the complexes. This suggest groove and/or electrostatic binding of the Cu(II) complex to CT DNA stabilizing the DNA double-helix structure in preference to an intercalative mode of binding to DNA that normally gives large positive ΔT_m values [87,88].

DNA Photocleavage studies

The ability of Co(II), Ni(II) and Cu(II) complexes to cleave supercoiled (SC) pUC19 DNA (0.5 μg) in Tris–HCl/NaCl buffer has been studied by incubating the complexes for 1 h at different concentrations (40–60 μM) and after photoexposure at 365 nm using agarose gel electrophoresis. The resulting electrophoretic pattern is shown in Fig. 6.

The electrophoretic pattern showed the formation of an open circular DNA (form II) and linear DNA (Form III) from the supercoiled DNA (form I) by the effect of various concentrations of the complexes (40–60 μM) on constant DNA concentration at 37 °C, it indicates that under similar experimental conditions, the complexes appreciably exhibits a time/concentration dependent DNA cleavage activity.

As presented in Fig. 6, no perceptible DNA cleavage was observed for negative control (lane 1). At the concentration of 40 μM of the Co(II), Ni(II) and Cu(II) complexes (lanes 5, 7 and 9), the amount of Form I of supercoiled DNA diminish gradually, with increase of nicked circular DNA (Form II) whereas, at the concentration of 60 μM, (lanes 6, 8 and 10) significant amounts of linear DNA (Form III) are clearly visible for all the complexes.

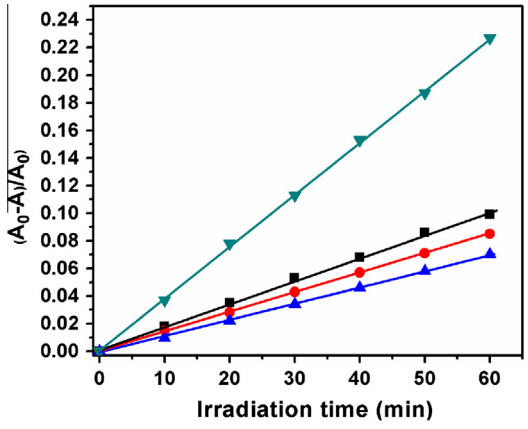

Fig. 7. The DPBF consumption percentage as a function of irradiation time in the air-equilibrated DMSO solution of Co(II) (●), Ni(II) (◄) and Cu(II) (■). $[Ru(bpy)_3]^{2+}$ (►) as standard ($\Phi_{\Delta s}$ = 0.81) in air equilibrated CH_3OH.

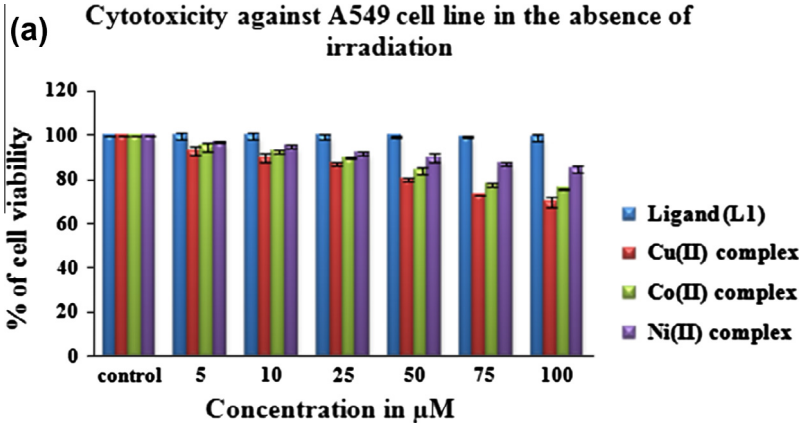

Fig. 8a. Cytotoxicity of Co(II), Ni(II) and Cu(II) complexes to A549 cells in the absence of irradiation.

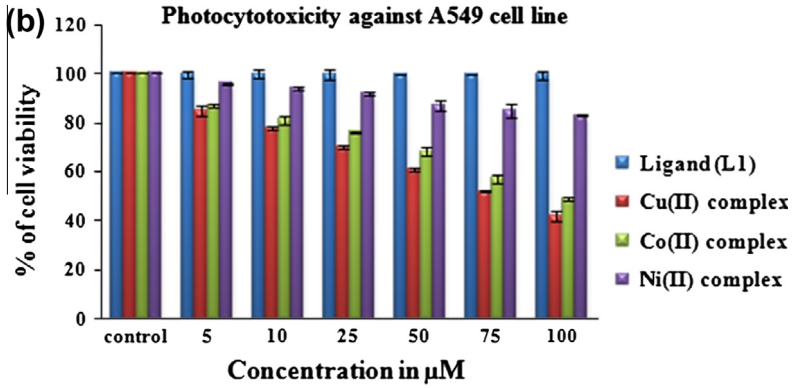

Fig. 8b. Cytotoxicity of Co(II), Ni(II) and Cu(II) complexes to A549 cells in the presence of irradiation.

The photocleavage activity of supercoiled (SC) pUC19 DNA at 365 nm, is expected to occur through the photoexcitation of the charge-transfer bands of the complexes, leading to the creation of an excited singlet state through the triplet state activates molecular oxygen to form reactive hydroxyl or singlet oxygen species. Experiments with different scavenging agents were carried out to identify the intermediate reactive oxygen species (ROS) that might be formed in the DNA cleavage reaction (Fig. 6). In order to witness the role of singlet oxygen in the cleavage pathway, an experiment was conducted in presence of sodium azide (NaN_3), a singlet oxygen quencher. The NaN_3 completely inhibited the cleavage reaction (lane 2) indicating $^1O_2$ generation plays a key role in photocleavage of pUC19 DNA. Hydroxyl radical scavenger, such as DMSO did not show any inhibitory effect, thus excluding the possibility of a type-I pathway forming hydroxyl radical (.OH) (lane 4). This can be further confirmed by testing the cleavage of supercoiled (SC) pUC19 DNA, in the presence of D_2O. Due to the longer lifetime of singlet oxygen in D_2O solvent the expected strand scission would be more in D_2O [89,90]. The formation of singlet oxygen is supplementary supported by the enhancement of the percentage of SC DNA cleavage in D_2O solvent (lane 3).

It is obvious from the above results that, the photocleavage activity of SC pUC19 DNA at 365 nm is much efficient in all the complexes studied. The motive for the enhanced cleavage ability of these complexes may be accredited to the generation of $^1O_2$ during the cleavage process.

Quantum yield of $^1O_2$ generation

Plentiful organic compounds can react with reactive oxygen species such as $^1O_2$, leading to the changes of absorbance and/or fluorescence intensity, and consequently can be utilized to quantitatively assess the $^1O_2$ generation quantum yields of photosensitizers by simply monitoring the fluorescence or UV–visible spectrum [91]. 1,3-Diphenylisobenzofuran (DPBF, Scheme 2) with a reported β value of about 10^{-4} is presently one of the most reactive with $^1O_2$. The consumptions of DPBF were followed by monitoring its loss of absorbance at 417 nm and be articulated as a function of photosensitizers $^1O_2$ generation quantum yield (Φ_Δ) according to the literature method [92,93]. Using $[Ru(bpy)_3]^{2+}$ as standard ($\Phi_{\Delta s} = 0.81$), the Φ_Δ of Co(II), Ni(II) and Cu(II) complexes in DMSO were determined to be 0.28, 0.25 and 0.30, respectively (Fig. 7), implying their prospective application in $^1O_2$-involving processes, such as photocleavage of DNA.

Anti-tumor study on A549 (lung carcinoma) cell

The cytotoxicity assays of Co(II), Ni(II) and Cu(II) complexes to human lung tumor cells of A549 were measured by MTT reduction assay [94]. Fig. 8a and b shows the result of the cell viability experiments intended at determining the dose dependent, dark cytotoxicity and photocytotoxicity of complexes to human lung carcinoma cells of A549.

In the present investigation, it was notable that the ligand was almost inactive against A549 cancer cell lines. However, all of the complexes exhibited considerable cytotoxic specificity towards the A549 cancer cell lines. At all concentration, in the absence of irradiation the complexes moderately reduced the viable A549 cells after staining with trypan blue at 72 h (effects on cell proliferation), which was slightly more at higher concentrations (50–100 μM) (Fig. 8a). Under similar experimental conditions but with irradiation, the complexes (except Ni(II)) show enhanced

cytotoxicity and reduced maximum number of viable A549 cells at both lower and higher concentrations (Fig. 8b). Furthermore, Cu(II) complex showed much superior antitumor activity to other complexes on A549 cell lines. The cytotoxicity displayed by Co(II) complex was similar with Cu(II) complex, but the Ni(II) complex exhibited negligible cytotoxicity towards A549 cancer cell lines. These results further support the conclusion reached by MTT reduction assay that these complexes showed considerable dose dependent cytotoxicity to A549 cells in presence of light irradiation. Hence, it can be concluded that the generation of $^1O_2$, upon light irradiation may account for the fine photocytotoxicity of these complexes.

Conclusion

In summary, three bivalent metal complexes of Schiff base ligand (L_1) have been synthesized and structurally characterized. In concurrence with UV–visible absorption, thermal denaturation and viscosity measurements, all the complexes display efficient DNA binding propensity. The observed intrinsic binding constant (K_b) together with structural analysis, imply a covalent mode of DNA binding for Co(II) and Ni(II) complexes and a surface binding to minor groove for Cu(II) complex. When irradiated by UV–visible light, the complexes are found to be proficient photocleaving agents of DNA. The mechanism reveals that the singlet oxygen ($^1O_2$) play an important role in the DNA photocleavage and possessed significant cytotoxic activities, especially Cu(II) complex had an obviously superior inhibitory rate than ligand (L_1) and other two complexes. Hence, these complexes may be useful as potential PDT agents in photochemical therapy.

Acknowledgments

Authors are thankful to Board of Research in Nuclear Sciences, Mumbai, INDIA for supported the work through a Major Research Project (No. 2009/34/44/BRNS/3227).

Appendix A. Supplementary material

Supplementary data associated with this article can be found, in the online version, at http://dx.doi.org/10.1016/j.saa.2013.06.009.

References

[1] M.E. Rodriguez, F. Morán, A. Bonansea, M. Monetti, D.A. Fernández, C.A. Strassert, V. Rivarola, J. Awruch, L.E. Dicelio, Photochem. Photobiol. Sci. 2 (2003) 988–994.
[2] J.C. Kennedy, R.H. Pottier, D.C. Pross, J. Photochem. Photobiol. B 6 (1990) 143–148.
[3] W.-H. Wei, Z. Wang, T. Mizuno, C. Cortez, L. Fu, M. Sirisawad, L. Naumovski, D. Magda, J.L. Sessler, Dalton Trans. 16 (2006) 1934–1942.
[4] J. Ma, J. Chen, M. Idowu, T. Nyokong, J. Phys. Chem. B 112 (2008) 4465–4469.
[5] L. Shi, B. Hernandez, M. Selke, J. Am. Chem. Soc. 128 (2006) 6278–6279.
[6] K. Ishii, M. Shiine, Y. Shimizu, S. Hoshino, H. Abe, K. Sogawa, N. Kobayashi, J. Phys. Chem. B 112 (2008) 3138–3143.
[7] I.J. Macdonald, T.J. Dougherty, J. Porphyr. Phthalocya. 5 (2001) 105–129.
[8] Y. Jung, S.J. Lippard, Chem. Rev. 107 (2007) 1387–1407.
[9] X. Wang, Z. Guo, Dalton Trans. 12 (2008) 1521–1532.
[10] M.H. Garcia, T.S. Morais, P. Florindo, M.F.M. Piedade, V. Moreno, C. Ciudad, V. Noe, J. Inorg. Biochem. 103 (2009) 354–361.
[11] C.-H. Wu, D.-H. Wu, X. Liu, G. Guoyiqibayi, D.-D. Guo, G. Lv, X.-M. Wang, H. Yan, H. Jiang, Z.-H. Lu, Inorg. Chem. 48 (2009) 2352–2354.
[12] E. Kim, P.T. Rye, J.M. Essigmann, R.G. Croy, J. Inorg. Biochem. 103 (2009) 256–261.
[13] R. Gao, D.G. Ho, B. Hernandez, M. Selke, D. Murphy, P.I. Djurovich, M.E. Thompson, J. Am. Chem. Soc. 124 (2002) 14828–14829.
[14] M. Selke, W.L. Karney, S.I. Khan, C.S. Foote, Inorg. Chem. 34 (1995) 5715–5720.
[15] M.R. Detty, S.L. Gibson, S.J. Wagner, J. Med. Chem. 47 (2004) 3897–3915.
[16] R. Bonnett, Chemical Aspects of Photodynamic Therapy, Gordon & Breach, London, UK, 2000.
[17] A.K. Patra, T. Bhowmick, S. Ramakumar, M. Nethaji, A.R. Chakravarty, Dalton Trans. 48 (2008) 6966–6976.
[18] P. Adao, J.C. Pessoa, R.T. Henriques, M.L. Kuznetsov, F. Avecilla, M.R. Maurya, U. Kumar, I. Correia, Inorg. Chem. 48 (2009) 3542–3561.
[19] V.X. Jin, S.I. Tan, J.D. Ranford, Inorg. Chim. Acta 358 (2005) 677–686.
[20] P. Liu, J.C. Shi, Q. Tong, Y. Feng, H. Huang, L. Jia, Inorg. Chim. Acta 362 (2009) 229–232.
[21] M.K. Taylor, K.D. Trotter, J. Reglinski, L.E.A. Beriouis, A.R. Kennedy, C.M. Spickett, R.J. Sowden, Inorg. Chim. Acta 361 (2008) 2851–2862.
[22] S. Rayati, N. Torabi, A. Ghaemi, S. Mohebbi, A. Wojtczak, A. Kozakiewicz, Inorg. Chim. Acta 361 (2008) 1239–1245.
[23] S. Dhar, D. Senapati, P.K. Das, P. Chattopadhyay, M. Nethaji, A.R. Chakravarty, J. Am. Chem. Soc. 125 (2003) 12118–12124.
[24] S. Dhar, A.R. Chakravarty, Inorg. Chem. 42 (2003) 2483–2485.
[25] S. Dhar, D. Senapati, P.A.N. Reddy, P.K. Das, A.R. Chakravarty, Chem. Commun. 19 (2003) 2452–2453.
[26] C. Gruning, H. Schmidt, D. Rehder, Inorg. Chem. Commun. 2 (1999) 57–59.
[27] I. Cavaco, J. Costa Pessoa, M.T.L. Duarte, R.T. Henriques, P.M. Matias, R.D. Gillard, J. Chem. Soc., Dalton Trans. 9 (1996) 1989–1996.
[28] I. Cavaco, J. Costa Pessoa, M.T.L. Duarte, R.D. Gillard, P. Matias, Chem. Commun. 11 (1996) 1365–1366.
[29] J. Costa Pessoa, I. Cavaco, I. Correia, M.T. Duarte, R.D. Gillard, R.T. Henriques, F.J. Higes, C. Madeira, I. Tomaz, Inorg. Chim. Acta 293 (1999) 1–11.
[30] J. Costa Pessoa, M.J. Calhorda, V. Felix, S. Gama, I. Correia, M.T. Duarte, S. Marcao, M.F.M. Piedade, I. Tomaz, J. Inorg. Biochem. 86 (2001) 188.
[31] J. Costa Pessoa, M.T. Duarte, R.D. Gillard, C. Madeira, P.M. Matias, I. Tomaz, J. Chem. Soc., Dalton Trans. 23 (1998) 4015–4020.
[32] R. Karmakar, C.R. Choudhury, S. Mitra, L. Dahlenburg, Struct. Chem. 16 (2005) 611–616.
[33] L.L. Koh, J.O. Ranford, W. Robinson, J.O. Svensson, A.L.C. Tan, D. Wu, Inorg. Chem. 35 (1996) 6466–6472.
[34] C.T. Yang, B. Moubaraki, K.S. Murray, J.D. Ranford, J.J. Vittal, Inorg. Chem. 40 (2001) 5934–5941.
[35] C.T. Yang, B. Moubaraki, K.S. Murray, J.J. Vittal, J. Chem. Soc., Dalton Trans. 5 (2003) 880–889.
[36] P.A.N. Reddy, M. Nethaji, A.R. Chakravarthy, Eur. J. Inorg. Chem. 7 (2004) 1440–1446.
[37] R. Pradhan, A.M. Thomas, A. Mukherjee, S. Dhar, M. Nethaji, A.R. Chakravarthy, Indian J. Chem., Sect. A 44A (2005) 18–26.
[38] P.K. Sasmal, A.S. Patra, M. Nethaji, A.R. Chakravarthy, Inorg. Chem. 46 (2007) 11112–11121.
[39] M.-Z. Wang, Z.-X. Meng, B.-L. Liu, G.-L. Cai, C.-L. Zhang, X.-Y. Wang, Inorg. Chem. Commun. 8 (2005) 368–371.
[40] M.C. Prabahkara, H.S. Bhojya Naik, Biometals 21 (2008) 675–684.
[41] B. Vinay Kumar, H.S. Bhojya Naik, D. Girija, N. Sharath, S.M. Pradeepa, H. Joy Hoskeri, M.C. Prabhakara, Spectrochim. Acta A 94 (2012) 192–199.
[42] C.N. Sudhamani, H.S. Bhojya Naik, T.R. Ravikumar Naik, M.C. Prabhakara, Spectrochim. Acta A 72 (2009) 643–647.
[43] S.M. Pradeepa, H.S. Bhojya Naik, B. Vinay Kumar, K. Indira Priyadarsini, Atanu Barik, T.R. Ravikumar Naik, Spectrochim. Acta Part A 101 (2013) 132–139.
[44] B. Vinay Kumar, H.S. Bhojya Naik, D. Girija, N. Sharath, S.M. Pradeepa, J. Macromol. Sci. Part A Pure Appl. Chem. 49 (2012) 139–148.
[45] J.B. Chaires, N. Dattagupta, D.M. Crothers, Biochemistry 21 (1982) 3933–3940.
[46] R. Augamuthu, V. Rajendiran, P. Umamaheshwari, R. Balamurugan, C.A. Kilner, M.A. Halcrow, M. Palaniandavar, J. Inorg. Biochem. 99 (2005) 1717–1732.
[47] Z. Hang, S.L. Chun, H.B. Xian, Y. Ming, J. Inorg. Biochem. 99 (2005) 1119–1125.
[48] M.C. Prabhakara, H.S. Bhojya Naik, V. Krishna, H.M. Kumaraswamy, Nucleos. Nucleot. Nucl. 26 (2007) 459–471.
[49] A.A. Abdel-Shafi, P.D. Beer, R.J. Mortimer, F. Wilkinson, J. Phys. Chem. A 104 (2000) 192–202.
[50] P. Zhang, J. Chen, Y. Liang, Acta Biochim. Biophys. Sin. 42 (2010) 440–449.
[51] Z.M. Zaki, G.G. Mohamed, Spectrochim. Acta A 56 (2000) 1245–1250.
[52] S.A. Patil, S.N. Unki, A.D. Kulkarni, V.H. Naik, P.S. Badami, J. Mol. Struct. 985 (2011) 330–338.
[53] M.P. Sathisha, U.N. Shetti, V.K. Revankar, K.S.R. Pai, Eur. J. Med. Chem. 43 (2008) 2338–2346.
[54] G. Singh, P.A. Singh, K. Singh, D.P. Singh, R.N. Handa, S.N. Dubey, Proc. Natl. Acad. Sci. Ind. 72A (2002) 87–94.
[55] B. Selvakumar, V. Rajendiran, P.U. Maheshwari, H. Stoeckli-Evans, M. Palaniandavar, J. Inorg. Biochem. 100 (2006) 316–330.
[56] T.N. Sorrel, Tetrahedron 45 (1989) 3–68.
[57] D.W. Smith, Coord. Chem. Rev. 21 (1976) 93–158.
[58] P.P. Hankare, S.R. Naravane, V.M. Bhuse, S.D. Delekar, A.H. Jagtap, Ind. J. Chem. 43A (2004) 1464–1467.
[59] T.R. Rao, P. Archan, Synth. React. Inorg. Metal.-Org. Chem. 35 (2005) 299–304.
[60] R.N. Patel, N. Singh, K.K. Shukla, U.K. Chauhan, S. Chakraborty, J. NiclosGutierrez, A. Castineiras, J. Inorg. Biochem. 98 (2004) 231–237.
[61] K.S. Bharathi, A.K. Rahiman, K. Rajesh, S. Sreedaran, P.G. Aravindan, D. Velmurugan, V. Narayanan, Polyhedron 25 (2006) 2859–2868.
[62] R.C. Santana, J.F. Carvalho, I. Vencato, H.B. Napolitano, A.J. Bortoluzzi, G.E. Barberis, R.E. Rapp, M.C.G. Passeggi, R. Calvo, Polyhedron 26 (2007) 5001–5008.
[63] A.A. Soliman, G.G. Mohamed, Thermochim. Acta 421 (2004) 151–159.
[64] E.B. Seena, Nancy Mathew, Mini Kuriakose, M.R. Prathapachandra Kurup, Polyhedron 27 (2008) 1455–1462.
[65] N. Ertan, P. Gurkani, Dyes Pigm. 33 (1997) 137–147.
[66] A. Sreekanth, M.R.P. Kurup, Polyhedron 22 (2003) 3321–3332.
[67] B.J. Hathaway, D.E. Billing, Coord. Chem. Rev. 5 (1970) 143–207.

[68] Q.L. Zhang, J.G. Liu, H. Chao, G.Q. Xue, L.N. Ji, J. Inorg. Biochem. 83 (2001) 49–55.
[69] N. Grover, T.W. Welch, T.A. Fairley, M. Cory, H.H. Thorp, Inorg. Chem. 33 (1994) 3544–3548.
[70] A. Oleksi, A.G. Blanco, R. Boer, J. Usón, J. Aymamí, A. Rodger, M.J. Hannon, M. Coll, Angew. Chem. Int. Ed. 45 (2006) 1227–1231.
[71] R.S. Kumar, S. Arunachalam, V.S. Periasamy, C.P. Preethy, A. Riyasdeen, M.A. Akbarsha, Polyhedron 27 (2008) 1111–1120.
[72] M. Vujčić, M. Lazić, M. Milenković, D. Sladić, S. Radulović, N. Filipović, K. Anđelković, J. Biochem. Mol. Toxicol. 25 (2011) 175–182.
[73] I. Meistermann, V. Moreno, M.J. Prieto, E. Moldrheim, E. Sletten, S. Khalid, P.M. Rodger, J.C. Peberdy, C.J. Isaac, A. Rodger, M.J. Hannon, Proc. Natl. Acad. Sci. USA 99 (2002) 5069–5074.
[74] C.J. Larson, G.L. Verdine, in: S.M. Hecht (Ed.), Bioorganic Chemistry Nucleic Acids, Oxford University Press, New York, 1996, pp. 324–346.
[75] J.M. Kelly, A.B. Tossi, D.J. Mcconnell, C. Ohuigin, Nucl. Acids Res. 13 (1985) 6017–6034.
[76] J.D. McGhee, P.H. von Hippel, J. Mol. Biol. 86 (1974) 469–489.
[77] M.T. Carter, M. Rodriguez, A.J. Bard, J. Am. Chem. Soc. 111 (1989) 8901–8911.
[78] G. Jones, P. Willett, R.C. Glen, A.R. Leach, R. Taylor, Mol. Biol. 267 (1997) 727–748.
[79] B. Norden, T. Tjerneld, Biopolymers 21 (1982) 1713–1734.
[80] G. Yang, J.Z. Wu, L. Wang, L.N. Ji, X. Tian, J. Inorg. Biochem. 66 (1997) 141–144.
[81] L.S. Lerman, J. Mol. Biol. 3 (1961) 18–30.
[82] G.A. Neyhart, N. Grover, S.R. Smith, W.A. Kalsbeck, T.A. Fairley, M. Cory, H.H. Thorp, J. Am. Chem. Soc. 115 (1993) 4423–4428.
[83] K.E. Reinert, Biochim. Biophys. Acta 319 (1973) 135–139.
[84] J. Liu, H. Zhang, C. Chen, H. Deng, T. Lu, L.N. Ji, J. Chem. Soc., Dalton Trans. 1 (2003) 114–119.
[85] E.T. Kalouli, N. Katsaros, J. Inorg. Biochem. 37 (1989) 271–282.
[86] J.P. Macquet, J.L. Butour, N.P. Johnson, ACS Symp. Ser. 209 (1983) 75–100.
[87] L.E. Gunther, A.S. Yong, J. Am. Chem. Soc. 90 (1968) 7323–7328.
[88] Y. An, S.-D. Liu, S.-Y. Deng, L.-N. Ji, Z.-W. Mao, J. Inorg. Biochem. 100 (2006) 1586–1593.
[89] A. Sitlani, E.C. Long, A.M. Pyle, J.K. Barton, J. Am. Chem. Soc. 114 (1992) 2303–2312.
[90] M.C. Prabhakara, B. Basavaraju, H.S. Bhojya Naik, Bioinorg. Chem. Appl. 2007 (2007) 1–7.
[91] H.Y. Ding, X.S. Wang, L.Q. Song, J.R. Chen, J.H. Yu, C. Li, B.W. Zhang, J. Photochem. Photobiol. A Chem. 177 (2006) 286–294.
[92] R.H. Young, K. Wehrly, R.L. Martin, J. Am. Chem. Soc. 93 (1971) 5774–5779.
[93] I.E. Kochevar, R.W. Redmond, Methods Enzymol. 319 (1992) 20–28.
[94] T. Mosmann, J. Immunol. Methods 65 (1983) 55–63.